EUROPEAN ORGANIZATION FOR NUCLEAR RESEARCH

CERN – SL DIVISION

chramp.tex **CERN-SL-2000-14 MS**

Proposal to Increase the LEP Energy with Horizontal Orbit Correctors

A. Beuret, S. Bidon, G. de Rijk, R. Genand, P. Raimondi, J. Wenninger

Abstract

In an $\mathrm{e^+e^-}$ collider the beam energy depends only on the bending field integral $\oint B\,ds$ while the synchrotron radiation power scales with $\oint B^2\,ds$ and is sensitive to the details of the field distribution. With fixed RF acceleration voltage it is thus possible to attain higher energies by increasing the effective bending magnet length. We propose to use the horizontal orbit correctors to exploit this effect. To control the orbit perturbations, 79 un-connected correctors in the regular arcs and 14 un-connected correctors in the dispersion suppressors will have to be powered. An energy increase of approximatively 0.18 GeV per beam might be obtained.

Geneva, Switzerland

January 2000

Contents

1 Introduction

In 1999 LEP ran at a beam energy as high as 101 GeV. This extraordinary achievement was entirely due to the superconducting RF system whose average gradient was pushed above 7 MV/m, significantly beyond the design figure of 6 MV/m. In order to raise the discovery (or exclusion) limit on the Higgs boson to the highest possible mass, the beam energy of LEP must be increased as much as possible using the available equipment. Since it is clear that RF gradients cannot be stretched forever, a proposal was made to increase the energy by spreading out the bending field using horizontal correctors or quadrupoles [1]. The schemes based on quadrupoles consisted in either displacing the magnets systematically or adding additional windings. Both proposals were finally dismissed due to the risk of damaging components. The focus of this report is therefore to propose a complete scheme of energy increase based on horizontal correctors.

2 Energy Increase by Bending Field Spreading

In a circular e^+ or e^- machine the beam energy E is to a very good approximation given by the integral on the magnetic field B

$$E = \frac{ec}{2\pi} \oint B\, ds = 47.7[\mathrm{MeV/Tm}] \oint B\, ds \tag{1}$$

with e the electron charge and c the speed of light. Contrary to the beam energy the energy loss from synchrotron radiation U_0 is sensitive to the details of the field distribution

$$U_0 = \frac{C_\gamma (ec)^2}{2\pi} \oint E^2\, B^2\, ds = \frac{C_\gamma}{2\pi} \oint \frac{E^4}{\rho^2} ds \tag{2}$$

where ρ is the local bending radius. The constant C_γ depends on the electron mass m_e and on the classical electron radius r_e

$$C_\gamma = \frac{4\pi\, r_e}{3\,(m_e c^2)^3} = 8.85 \cdot 10^{-5} \mathrm{m/GeV}^3 \tag{3}$$

Integration of Equation 2 yields an expression for U_0 in terms of the effective bending radius $\bar{\rho}$

$$U_0 = C_\gamma \frac{E^4}{\bar{\rho}} \tag{4}$$

It is clearly possible to reduce the energy loss by spreading out the bending field thereby increasing $\bar{\rho}$. For a fixed total RF acceleration voltage V_{RF} it is thus possible to increase the beam energy. This fact was already used at the design phase of LEP to define the size of the machine and of the RF system [2, 3].

We consider now a machine with bending magnets and horizontal orbit correctors and neglect for the moment the effects of orbit distortions. In this case we can express E and U_0 as

$$E = \frac{ec}{2\pi}(B_d L_d + B_c L_c) \tag{5}$$

$$U_0 = \frac{C_\gamma (ec)^2}{2\pi} E^2 (B_d^2 L_d + B_c^2 L_c) \tag{6}$$

B_d is the field and L_d the total (magnetic) length of the dipole magnets. B_c and L_c are the corresponding quantities for the corrector magnets. Under the assumption that $B_c L_c << B_d L_d$ and that U_0 is the only relevant quantity that must be kept constant, the highest beam energy that can be achieved for a given RF voltage V_{RF} is :

$$E \simeq E_0 \left(1 + \frac{1}{2}\frac{B_c L_c}{B_d L_d}\left(1 - \frac{1}{2}\frac{B_c}{B_d}\right)\right) \tag{7}$$

Magnet Type	Parameter	Value
Dipole	Magnetic length L_d	19.2 km
	Magnetic field B_d at 100 GeV	0.107 T
	Integrated field $B_d L_d$ at 100 GeV	2092 Tm
MCH Corrector	Magnetic length L_c	0.51 m
	Maximum field B_c^{max}	0.057 T
	Maximum integrated field/magnet $B_c^{max} L_c$	0.0311 Tm
	Maximum deflection/magnet θ^{max}	93 μrad
	Maximum current I^{max}	2.5 A
MCHA Corrector	Magnetic length L_c	0.51 m
	Maximum field B_c^{max}	0.071 T
	Maximum integrated field/magnet $B_c^{max} L_c$	0.0393 Tm
	Maximum deflection/magnet θ^{max}	118 μrad
	Maximum current I^{max}	5.0 A

Table 1: Magnet parameters at 100 GeV. The LEP regular arc cells are equipped with MCH correctors. There are 31 arc cells per octant. The MCHA correctors are installed in the dispersion suppressors and insertions.

E_0 is the maximum energy that can be reached when $B_c = 0$ and only the dipoles are used to define the beam energy. Provided that B_c is not too high the total beam energy can be increased by *spreading* the bending over more magnets. This argument is of course equally valid for other types of magnets. We will refer to this method with the acronym **BFS** (Bending Field Spreading).

The parameters of the dipoles and the correctors for a nominal beam energy of 100 GeV are given in Table 1. Since a margin of 20 μrad must be foreseen for orbit steering, the maximum available deflection Θ_{bfs} that can be used for field spreading is 70 μrad per MCH correctors. At this strength the field in the correctors is B_c = 0.043 T for a total integrated field of $B_c L_c \simeq$ 6.5 Tm. Since in this case $B_c/B_d \simeq 1/2$, the energy gain ΔE that can be obtained when all arc and dispersion suppressor correctors are powered is

$$\Delta E = E - E_0 \simeq E_0 \, \frac{3}{8} \, \frac{B_c L_c}{B_d L_d} \simeq 120 \text{ MeV} \tag{8}$$

This gain can only be achieved if the presently unused correctors in the LEP arcs are also powered. For the arc corrector configuration that was available up to 1999 the maximum gain is approximatively 30% lower.

For this simple estimate side effects due to orbit distortions were neglected. In general this cannot be done since :

- "Incoherent" orbit distortions may induce large additional energy losses in the quadrupoles leading to a significant reduction of the energy gain.
- "Coherent" orbit shifts in the quadrupoles may increase the gain if the deflections add up.
- The orbit shifts may change the damping partition numbers.

A precise estimate of the energy gain must must be evaluated from the quantum lifetime τ_q which does not only depend on U_0. The expression for τ_q is [4]

$$\tau_q = \frac{\tau_E}{n_\sigma^2} \, e^{n_\sigma^2/2} \tag{9}$$

with τ_E the longitudinal damping time. n_σ is the ratio between the RF bucket height and the energy

spread of the beam which is given by

$$n_\sigma^2 = \frac{2\,E\,U_0}{\pi\,\alpha\,h\,\sigma_E^2}(\frac{\pi}{2} - \phi_s - \cot\phi_s) \tag{10}$$

τ_q is a steep function of n_σ which does not only depend on the energy loss but also on the momentum compaction factor α and the beam energy spread σ_E. h is the harmonic number of the RF system and ϕ_s the stable phase angle

$$\sin\phi_s = \frac{U_0}{V_{RF}} \tag{11}$$

The maximum beam energy and τ_q are only determined by U_0 for a given RF voltage V_{RF} as long as α and σ_E remain constant. In fact σ_E follows the approximate scaling law [4]

$$\sigma_E^2 \sim \frac{E^4}{\rho_0} \tag{12}$$

for a machine with constant bending radius ρ_0. Although this relation is no longer exact when the bending radius varies along the machine as is the case with BFS, it indicates that σ_E is likely to go down and that some additional corrections to the estimate from Equation 8 may be required. The horizontal beam emittance ε_x scales approximatively like

$$\varepsilon_x \sim \frac{\alpha E^2}{\rho_0} \tag{13}$$

and will also be affected by BFS.

3 Missing Correctors and Closed Orbits

The LEP arcs are designed with one horizontal corrector next to each horizontally focusing quadrupole (QF) and one vertical orbit correctors next to each vertically focusing quadrupoles (QD). During the construction of LEP only 169 horizontal correctors (MCH) were connected to a power converter. In the regular arcs one out of three horizontal correctors was not connected (79 in total). The magnets were installed but no PC was connected. As each corrector should be individually powered this meant a considerable saving on PCs and cables. We will denote the present situation of LEP with the 79 unused MCH correctors as the '2-in-3 scheme'.

The missing deflections cause important orbit distortions when all MCH are set to $\Theta_{bfs} = -50\,\mu rad$ (at LEP by convention negative corrector kicks correspond to deflection towards smaller radii). In Figure 1 the present situation is compared to the ideal situation where all arc correctors are powered (the '3-in-3 scheme'). The raw closed orbit RMS at the quadrupoles reaches 6 mm and is 4 times as large as for the case of one corrector per cell. The orbit distortion cannot be corrected completely as one must compensate a large missing kick every third cell. The additional energy losses due to the orbit offsets in the quadrupoles almost completely cancels the gain due to field spreading. A poor orbit steering in the even points may also lead to increased backgrounds in the LEP experiments.

It is clearly desirable to use all arc correctors in the machine, but the presently unused correctors need not be powered individually. 77 MCH arc correctors will be powered in series. Two correctors (CH.QF21.R1 and CH.QF21.L1) will be powered individually for technical reasons. More than 20 arc corrector magnets must first be re-installed. They had been replaced with (presently unused) skew quadrupoles in the first year of LEP to correct the coupling due to the Nickel layer on the vacuum chamber. Since some standard power converters are still available, the remaining 14 unused horizontal correctors in the dispersion suppressors will also be powered to improve orbit steering. A list is given in Table 2. Only the new MCHA correctors next to the QL15 quadrupoles will be equipped with a standard

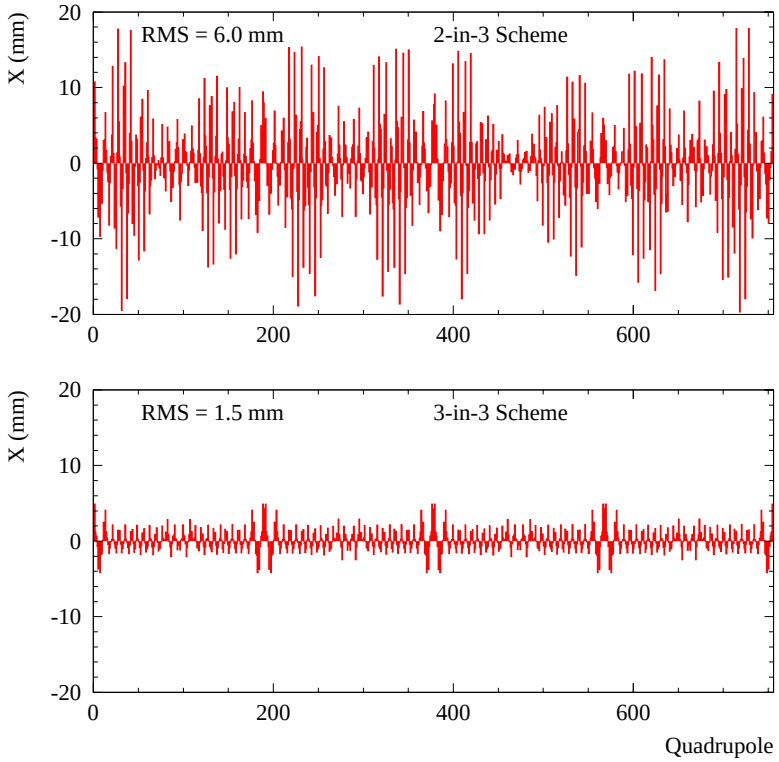

Figure 1: Simulated closed orbit at each quadrupole for the $102°/90°$ optics when all MCH correctors in the regular arc cells are set to $\Theta_{bfs} = -50\,\mu rad$. The upper figure corresponds to the situation with only 2 out of 3 cells equipped with correctors ('2-in-3 scheme'), the lower figure is for the case with one corrector in every cell ('3-in-3 scheme').

IP	Magnet Name	I^{max} (A)	Optics Name	MAD Strength	Comment
1	MCHA135	5.0	CHA.QL15.L1	KCHA15.L1	
	MCHA165	5.0	CHA.QL15.R1	KCHA15.R1	
	MCH129	2.5	CH.QF21.L1	KCH21.L1	Arc corrector
	MCH171	2.5	CH.QF21.R1	KCH21.R1	Arc corrector
2	MCH232	2.5	CH.QS17.L2	KCH17.L2	
	MCH268	2.5	CH.QS17.R2	KCH17.R2	
3	MCHA335	5.0	CHA.QL15.L3	KCHA15.L3	
	MCHA365	5.0	CHA.QL15.R3	KCHA15.R3	
	MCHA333	2.5	CHA.QL17.L3	KCHA17.L3	
	MCHA367	2.5	CHA.QL17.R3	KCHA17.R3	
6	MCH632	2.5	CH.QS17.L6	KCH17.L6	
	MCH668	2.5	CH.QS17.R6	KCH17.R6	
7	MCHA735	5.0	CHA.QL15.L7	KCHA15.L7	
	MCHA765	5.0	CHA.QL15.R7	KCHA15.R7	
	MCHA733	2.5	CHA.QL17.L7	KCHA17.L7	
	MCHA767	2.5	CHA.QL17.R7	KCHA17.R7	

Table 2: List of the 14 new correctors for the dispersion suppressors and the 2 new individually powered arc correctors. With the exception of the correctors next to QS17 in points 2 and 6, all magnets are already installed and must only be powered.

5 A PC because they must be able to provide a large kick for BFS. The other correctors will be powered using 2.5 A PCs which leaves enough margin for BFS and normal orbit steering. Next to quadrupoles QS17 in points 2 and 6, the obsolete skew quadrupoles will be replaced by MCH instead of MCHA correctors in order to maximize the kick strength with the 2.5 A PCs.

The QS15 quadrupoles around all even points (space occupied by an off-momentum collimator) and the QL13 quadrupoles around IP3 (space occupied by a secondary aperture collimator) will then be the only remaining horizontally focusing quadrupoles of the LEP arcs and dispersion suppressors without horizontal corrector.

4 Bending Field Spreading Experiments

During the 1999 LEP run the principle of BFS was tested with the presently available '2-in-3 scheme'. The experiments were performed at injection for the $60°/60°$ and $102°/90°$ optics. In Figure 2 the closed orbit shifts due to an excitation of the horizontal correctors of $\Theta_{bfs} = -10\,\mu rad$ is compared to MAD predictions. For both optics the corrector excitation could be increased to $\Theta_{bfs} = -50\,\mu rad$ without particular difficulties, but the tunes and the horizontal orbits required important corrections. Figure 3 shows the closed orbit shift and the corrector settings change when Θ_{bfs} is set to $-50\,\mu rad$ and the orbit corrected for the $102°/90°$ optics. The orbit RMS at the monitors can be brought down below 1 mm, but the corrector pattern in the arcs is strongly perturbed by the correction. Instead of the nominal value of $-50\,\mu rad$ some correctors must be pushed to $-60\,\mu rad$ while others must be reduced below $-40\,\mu rad$.

The expected and measured tune shifts are compared in Table 3 and are in good agreement. Large negative tune shifts were observed, as expected for a increase in beam energy. From the agreement between MAD and data one should be confident that predictions for energy gains obtained from MAD can be trusted at least at the 10% level.

Optics	Θ_{bfs}	Orbit		ΔQ_h		ΔQ_v	
	(μrad)	Condition	RMS (mm)	Measured	Expected	Measured	Expected
$60°/60°$	-10	Uncor.	0.51	-0.026	-0.030	-0.034	-0.034
$102°/90°$	-10	Uncor.	0.75	-0.072	-0.069	-0.090	-0.085
$102°/90°$	-50	Corrected	0.88	-0.215	-0.253	-0.325	-0.345

Table 3: Comparison of measured and expected tune shifts ΔQ_h and ΔQ_v when the horizontal correctors are excited for the $60°/60°$ and $102°/90°$ optics. For an excitation $\Theta_{bfs} = -10\,\mu rad$ the comparison is made for uncorrected orbits. For $\Theta_{bfs} = -50\,\mu rad$ the expected tune change is calculated using the same corrector setting change as in the experiment, including the corrections to control the horizontal orbit. The larger tune trims on the $102°/90°$ optics are due to the much larger uncorrected (natural) chromaticities. The negative tune shifts reflect the increase of the beam energy.

5 Bending Field Spreading for the Final LEP Run

The complete BFS scheme for the final LEP run in 2000 includes powering all unused correctors in the arcs and dispersion suppressors. The dispersion suppressor correctors are powered individually while the MCH correctors are powered by octants.

5.1 Orbit Correction and Damping Partition Numbers

The uncorrected orbit at the quadrupoles was shown in Figure 1. With the regular arc pattern and the additional MCHA correctors the orbit can be corrected very easily. Figure 4 shows the corrected orbit at the quadrupoles and the corresponding corrector trims when all MCH are excited to $-70\,\mu rad$. The

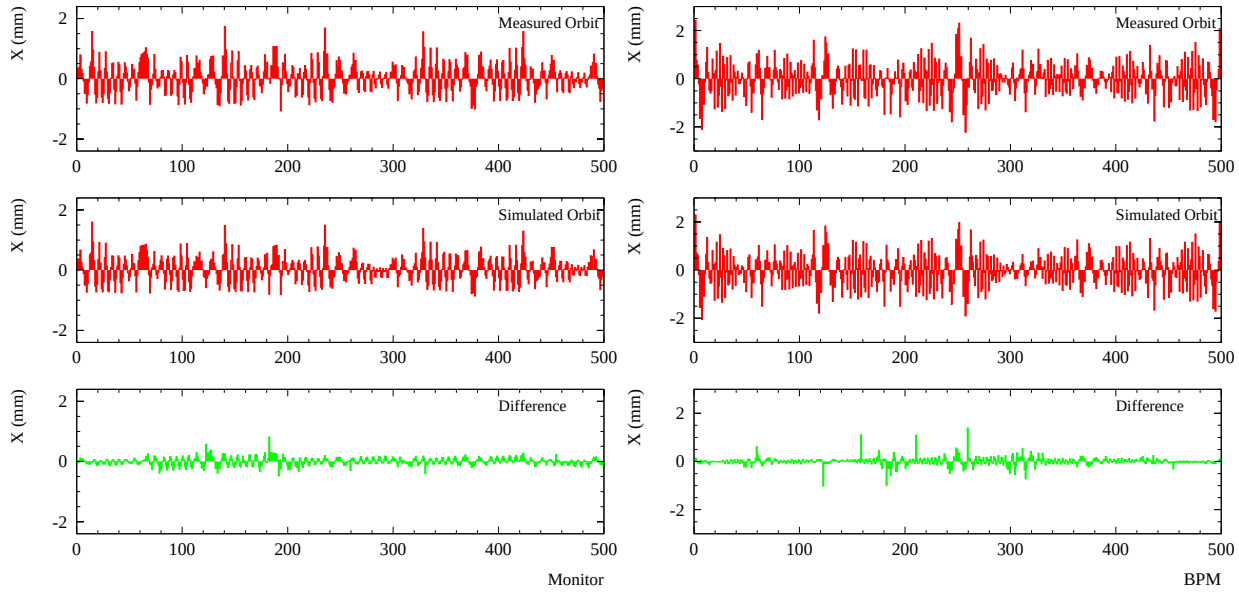

Figure 2: Comparison of measured and predicted closed orbit shifts with the $60°/60°$ (left) and $102°/90°$ (right) optics when the existing MCH are excited to $\Theta_{bfs} = -10\,\mu rad$.

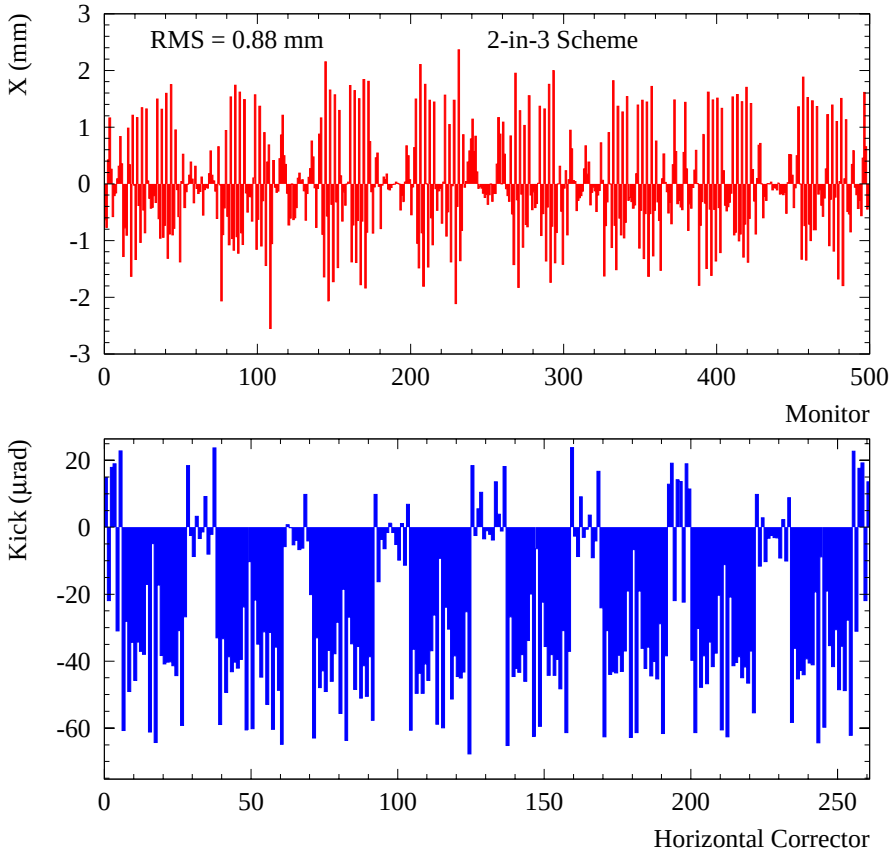

Figure 3: Measured closed orbit shift and change in horizontal corrector setting *after* correction of the closed orbit when the MCH correctors are pushed to $\Theta_{bfs} = -50\,\mu rad$ with a '2-in-3 scheme'. The raw (uncorrected) orbit shift is shown in Figure 1. Due to the orbit correction a large number of correctors have to be set to values significantly different for the nominal setting of $-50\,\mu rad$.

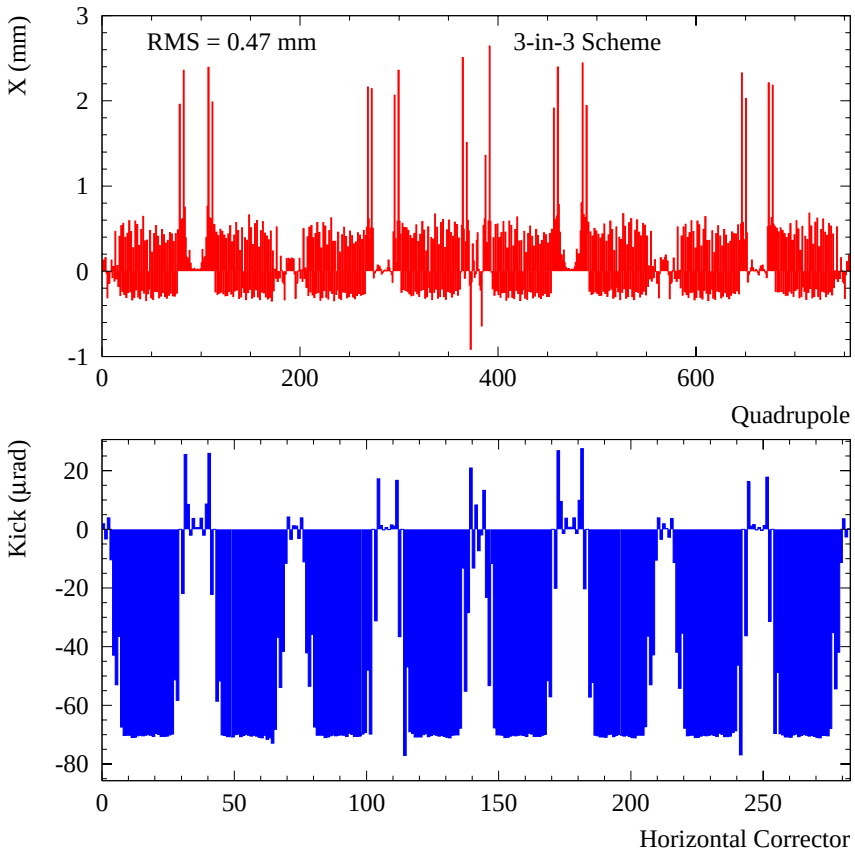

Figure 4: Corrected orbit at the quadrupoles (top) and final corrector settings change (bottom) for the $102°/90°$ optics with $\Theta_{bfs} = -70\,\mu rad$ when all correctors are powered. Only kicks of the individually powered corrected are shown. The orbit excursions of up to 2.3 mm are located in the dispersion suppressors of points 2,4,5,6 and 8 and are due to missing correctors (space occupied by collimators).

orbit was corrected with a Singular Value Decomposition algorithm using only individually powered correctors. The best correction is obtained by adding "virtual" monitors at all QF quadrupoles to the existing beam position monitors at the QD quadrupoles. This prevents biasing the orbit inside the QD quadrupoles. The overall orbit RMS is 0.47 mm, with peaks of $+2.3$ mm in the dispersion suppressors of points 2, 4, 5, 6 and 8. The orbit peaks are due to the missing correctors at quadrupoles QS15 and QL13. In the even straight sections the orbit is well corrected, an important requirement to maintain good backgrounds in the LEP detectors.

In the arcs the orbit has a characteristic pattern, similar to an off-momentum orbit, the beam being off-centre to the outside in the QF quadrupoles and to the inside in the QD quadrupoles as shown in Figure 5. In such a configuration both QF and QD quadrupoles amplify the effect of the correctors. The deflection of the beam passing with a position offset x in a quadrupole of strength K and length l is $\theta_q = Klx$. For the $102°/90°$ optics $|Kl| \simeq 0.035\,\mathrm{m}^{-1}$ for both QF and QD quadrupoles, yielding a total kick $\theta_{QF} + \theta_{QD}$ of $\approx -27\,\mu rad$ per cell for $\Theta_{bfs} = -70\,\mu rad$. Because the field in the quadrupoles is much lower than the field in the dipoles, the energy gain is increased by approximatively 50%.

The systematic movement of the orbit in the quadrupoles modifies the horizontal and longitudinal damping partition numbers J_x and J_s :

$$J_x = 1 - \Delta \qquad\qquad J_s = 2 + \Delta \tag{14}$$

where Δ can be approximated by

$$\Delta \simeq \frac{\bar{\rho}}{\pi} \oint D_x \frac{K}{\rho} ds \tag{15}$$

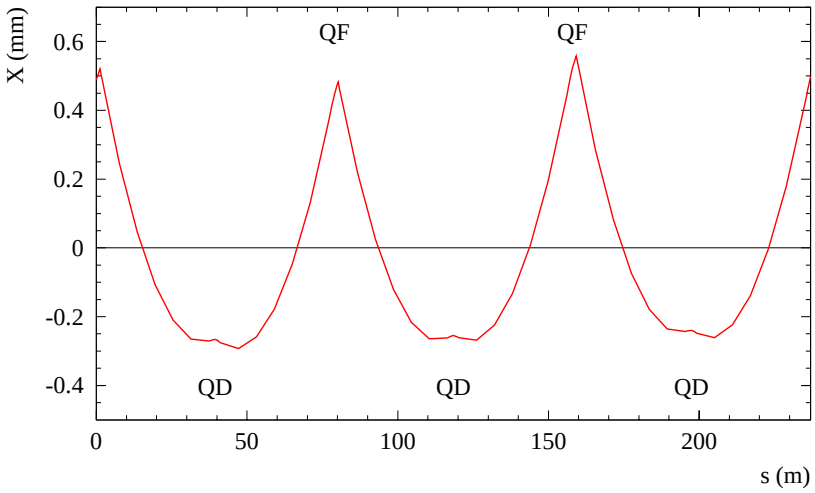

Figure 5: Corrected orbit over 3 arc cells for the $102°/90°$ optics with $\Theta_{bfs} = -70\,\mu rad$ when all correctors are powered (see also Figure 4). The orbit follows a characteristic "cusp shape" peaking in the QF quadrupoles. The beam is "launched" in the QF with a large inward angle that progressively changes sign over one cell because the beam is off-momentum with respect to the dipoles.

D_x is the horizontal dispersion and ρ is the local bending radius. Since for a beam offset x, $\rho \simeq 1/(Kx)$ in a quadrupole, Equation 15 becomes

$$\Delta \simeq \frac{\bar{\rho}}{\pi} \sum_i K_i^2 l_i D_{x,i} x_i \tag{16}$$

where the sum runs over all quadrupoles. In the arcs $K^2 l$ is almost identical for the QD and QF quadrupoles, but $(D_x x)_{QF} + (D_x x)_{QD} > 0$ which leads to a reduction of J_x. J_x scales with Θ_{bfs} since

$$J_x \sim x_i \sim \Theta_{bfs} \tag{17}$$

The orbit pattern visible in Figure 5 transforms the LEP arcs into a very weak but also very long "wiggler".

5.2 Energy Gain

The precise energy gain at high energy must be estimated with MAD. All estimates are made for a reference beam energy before BFS of 100 GeV. To clarify the influence of the various parameters, we will proceed in steps.

In a first step the energy gain from BFS is evaluated under the conditions that only the energy loss U_0 must remain constant. The prediction can then be directly compared with the estimates made in Section 2. In Table 4 the maximum beam energy E_f obtained from MAD is given for a machine with and without BFS. The net energy gains are 135 MeV for $\Theta_{bfs} = -50\,\mu rad$ and 176 MeV for $\Theta_{bfs} = -70\,\mu rad$. The last value is in good agreement with the simple estimate of 120 × 1.5 = 180 MeV obtained from Equation 8 when the 50% increase from the quadrupoles is taken into account. The systematic orbit distortion increases the horizontal emittances by approximatively 10% due to the reduction of J_x.

A better evaluation of the real energy gain is therefore obtained using as constraint that the energy loss U_0 and the damping partition number J_x should remain constant when BFS is applied. The results are given in Table 5. The net energy gains are now 123 MeV for $\Theta_{bfs} = -50\,\mu rad$ and 159 MeV for $\Theta_{bfs} = -70\,\mu rad$. Under those conditions the horizontal emittance ε_x, the energy spread σ_E and the

Θ_{bfs}	-	$-50\,\mu rad$	$-70\,\mu rad$
Dipole Energy E_d (GeV)	100.000	99.825	99.742
Total Energy E_f (GeV)	100.000	100.135	100.176
$(E_f - E_d)/E_d$ (%)	-	0.31	0.44
Net Energy Gain (MeV)	-	**135**	**176**
Energy Loss/turn U_0 (MeV)	2927.5	2927.6	2927.5
Hor. Damping Part. Number J_x	1.00	0.92	0.89
Hor. Emittance ε_x (nm)	44.5	47.9	49.3
Energy Spread σ_E (MeV)	157.4	153.9	152.6
Mom. Compaction factor α ($\times 10^4$)	1.557	1.550	1.546

Table 4: Energy gain and machine parameters with Θ_{bfs} set to 0 (no BFS), $-50\,\mu rad$ and $-70\,\mu rad$. The energy gains are obtained using as constraint a constant energy loss U_0.

Θ_{bfs}	-	$-50\,\mu rad$	$-70\,\mu rad$
Dipole Energy E_d (GeV)	100.000	99.839	99.762
Total Energy E_f (GeV)	100.000	100.123	100.159
$(E_f - E_d)/E_d$ %	-	0.28	0.40
RF Frequency Shift Δf_{RF} (Hz)	-	14.5	20.2
Net Energy Gain (MeV)	-	**123**	**159**
Energy Loss/turn U_0 (MeV)	2927.5	2927.7	2927.6
Hor. Damping Part. Number J_x	0.998	0.998	0.998
Hor. Emittance ε_x (nm)	44.5	43.9	43.7
Energy Spread σ_E (MeV)	157.4	156.9	156.6
Mom. Compaction factor α ($\times 10^4$)	1.557	1.550	1.546

Table 5: Energy gain and machine parameters with Θ_{bfs} set to 0 (no BFS), $-50\,\mu rad$ and $-70\,\mu rad$. The energy gains are obtained using as constraint a constant energy loss U_0 and a constant horizontal damping partition number J_x. Δf_{RF} is the RF frequency shift that is required to maintain J_x constant.

Θ_{bfs}	-	$-50\,\mu rad$	$-70\,\mu rad$
Dipole Energy E_d (GeV)	100.000	99.860	99.790
Total Energy E_f (GeV)	100.000	100.144	100.187
$(E_f - E_d)/E_d$ %	-	0.28	0.40
RF Frequency Shift Δf_{RF} (Hz)	-	14.5	20.2
Net Energy Gain (MeV)	-	**144**	**187**
Energy Loss/turn U_0 (MeV)	2927.5	2930.2	2930.9
Hor. Damping Part. Number J_x	0.998	0.998	0.998
Hor. Emittance ε_x (nm)	44.5	44.0	43.7
Energy Spread σ_E (MeV)	157.4	157.0	156.8
Mom. Compaction factor α ($\times 10^4$)	1.557	1.550	1.546

Table 6: Energy gain and machine parameters with Θ_{bfs} set to 0 (no BFS), $-50\,\mu rad$ and $-70\,\mu rad$. The energy gains are obtained using as constraint a constant quantum lifetime and a constant horizontal damping partition number J_x. Δf_{RF} is the RF frequency shift that is required to maintain J_x constant.

momentum compaction factor α decrease with BFS. This behaviour is expected from the dependence of those parameter on the bending radius as was pointed out in Section 2.

The smaller values of α and σ_E indicate that there is still room for energy increase since in the condition of Table 5 the quantum lifetime is higher with BFS : for identical τ_q the RF voltage margin increases by 4 MV for $\Theta_{bfs} = -70\,\mu rad$. In Table 6 the best estimate for the energy gain is finally evaluated using a constant J_x and τ_q. The final values for energy gains are 123 MeV for $\Theta_{bfs} = -50\,\mu rad$ and 187 MeV for $\Theta_{bfs} = -70\,\mu rad$.

5.3 Beam Optics

To preserve the beam optics the quadrupole and sextupole strengths must be increased proportionally to the difference between the dipole energy and the total energy ($(E_f - E_d)/E_d$ in Table 4). The vertical betatron function β_y^* at the even collision points requires a small additional correction to prevent it shifting from 5.0 cm down to 4.0 cm. The origin of this β_y^* reduction lies in the perturbation of the optics due the beam offsets in the sextupoles (Figures 4 and 5). An overall tune correction must also be applied. Following all those manipulations and corrections the betatron function beating is negligible in the horizontal and smaller than about 7% in the vertical plane as shown in Figure 6.

The change of the horizontal dispersion due to BFS is shown in Figure 7. The dispersion change is small, but one can observe a reduction of the average dispersion that reflects the change of bending radius and the contribution of the quadrupoles. This effect is related to the reduction of the momentum compaction factor in Tables 4 to 6.

6 Side Effects of Bending Field Spreading on Correctors

The use of BFS has consequences for orbit correction, collimator settings and energy calibration.

6.1 Orbit Correction

There are two implication of BFS for *horizontal* orbit corrections :

- The large kicks required for BFS limit the available range for steering. The maximum value for Θ_{bfs} will have to be selected after evaluation of the needs for good steering. Experience from previous years indicates that a margin of $20\mu rad$ is sufficient for steering.
- *Bare orbit corrections* will no longer be possible in the horizontal plane because the unfolding of the corrector kicks using the usual response for "incoherent" kicks is not valid.

6.2 Collimation

The orbit bumps around the even IPs visible in Figure 4 move the beams *away* from the off-momentum collimator jaws next to quadrupole QS17 by 1.5 to 2 mm. This corresponds approximatively to $1\,\sigma$ in beam size under physics conditions. This effect can be handled by a simple adjustment of the collimator files, eventually providing files valid when BFS is used or not. The setting of the off-momentum collimators is usually not very critical. At the secondary horizontal aperture collimator next to quadrupole QL13 the orbit movement can be neglected.

6.3 Energy Calibration

For beam energy calibration the first objective will be to measure precisely the energy change due to the correctors and quadrupoles. There are 2 simple choices.

- The energy change can be measured in physics condition using the LEP Spectrometer by determining the angle change when BFS is applied.

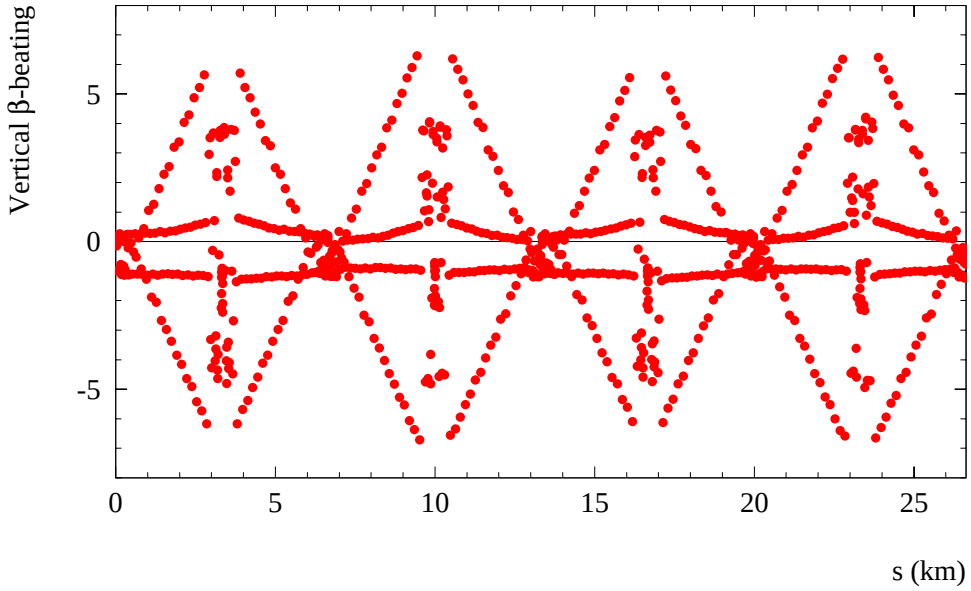

Figure 6: Vertical betatron function beating in % induced on the $102^\circ/90^\circ$ optics with $\Theta_{bfs} = -70\,\mu rad$ ('3-in-3 scheme').

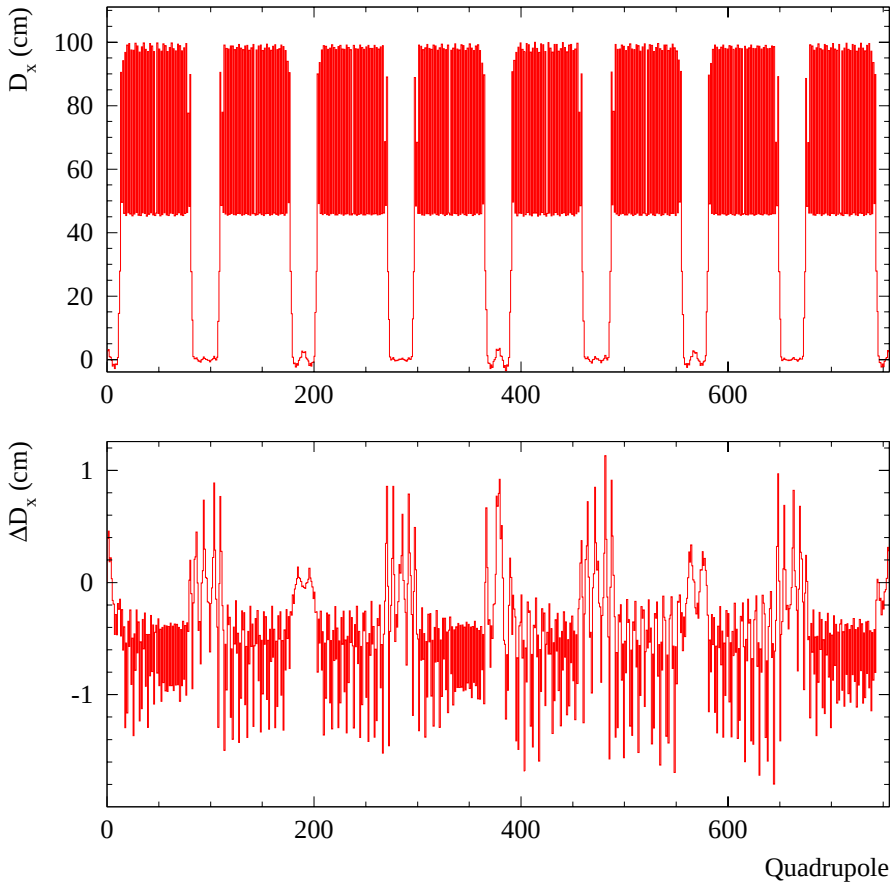

Figure 7: Horizontal dispersion D_x at the quadrupoles (top) and difference with respect to the nominal dispersion (bottom) for $\Theta_{bfs} = -70\,\mu rad$ using the '3-in-3 scheme'. The average dispersion is reduced due to the increase of $\bar{\rho}$

- At 45 GeV resonant depolarization can also be used to determine very precisely the energy change. This has however the disadvantage that small changes between 45 GeV and top energy cannot be accounted for.

Besides the task of measuring the energy change, BFS also brings along some complications.

- The Spectrometer beam position monitors are presently calibrated using bump scans. Such scans were already difficult at top energies in 1999 due to the large kicks ($\approx 80\mu rad$) that are required to move the beams. With BFS it will not longer be possible to perform such scans parasitically during physics. It should however be possible to remove BFS at an end of fill for Spectrometer calibration purposes. On the other hand those bump calibrations are mainly used during dedicated energy calibration runs where BFS will not have to be used.
- The central frequency measurement may be affected by the systematic offsets of the beams in quadrupoles and sextupoles. The precise impact will have to be studied. The systematic shift of the beam at the beam position monitors will require important corrections for the measurement of the average beam position at the arc quadrupoles which is used to track the ring circumference on a fill by fill basis.

7 Operational Procedure

The increase in energy obtained from BFS is only needed for physics runs and at the highest energies when the RF voltage is a limiting factor. To be flexible BFS should be used in the form of a "knob" that can be added at the end of the normal ramp when the machine is prepared for physics. The knob must include :

- The corrector trims including Θ_{bfs} and the associated orbit correction (see for example Figure 4).
- A strength change of the quadrupoles and sextupoles to match the new final energy.
- A small correction of β_y^*.
- A chromaticity trim.
- An overall tune correction.

The BFS knob must be applied at the end of the normal ramp when the machine is prepared for physics. The horizontal orbit must already be clean (i.e. no exceesively large kicks). With BFS the machine can still ne ramped using the mini-ramp functionality. The highest setting of the dipoles E_d should be set approximatively 0.2 GeV (see Table 6) below the maximum energy that can be achieved without BFS. Appropriate sofware for this knob must be developed during the 1999/2000 shutdown. For technical reasons the nominal beam energy, which also appears on the LEP page1 video channel, will remain set to E_d.

8 Connection of the Unused Horizontal Correctors

LEP was designed to be able to run with a $60°/60°$ optics for LEP1. This implied providing a bus-bar system for 2×3 families of sextupoles. For the presently used $102°/90°$ optics only 2×2 families are used. There are thus two bus bar systems available in the ring. The bus bars can be connected to a power converter in the even points dividing the machine into quadrants. Using the cables of the obsolete octupole magnets we can further divide the system in 8 circuits. The MCH magnets have a resistance of 23Ω, the cables and bus-bars a resistance of 2Ω. The voltage required for the 2.5 A current is 580 V for $\frac{1}{8}^{th}$ of the machine. To avoid extra costs in the injection areas two MCH magnets will be put on an individual power converter (CH.QF21.L1 and CH.QF21.R1, see Table 2).

8.1 Power convertors

No standard LEP power convertor can be used for the 8 corrector circuits, but the new NO2 power convertors, intended for the SPS transfer lines upgrade, could be modified for this purpose since they can supply up to 700 V. Their installation in the SPS will have to be postponed until October 2000 after the LEP shut-down. The controls electronics has to be interfaced to LEP standard crates. The LEP standard crates can be recuperated from the unused LEP octupole circuits. This adaption requires development work by a CERN staff engineer. The actual installation can be done by contract personnel.

8.2 Hardware work

Figure 8 shows the circuits of the MCH magnets to be connected. The two MCH correctors next to QF21 on both sides of point 1 will be equipped with individual PCs because they cannot be connected to the bus-bars. The work to be done for the connection of the other unused MCH correctors is:.

- Connect the octupole cables to the bus-bars for each $\frac{1}{8}^{th}$ of the machine.
- Connect the regular arc MCH magnets to the bus-bar.
- Connect the MCH magnets in the injection areas to the bus-bar.
- Modify the power convertors to the LEP standard.
- Install the 8 power convertors in the 4 SR buildings.
- Install $50Hz$ power for the power convertors in the 4 SR buildings.
- Connect power convertors and test the circuits.

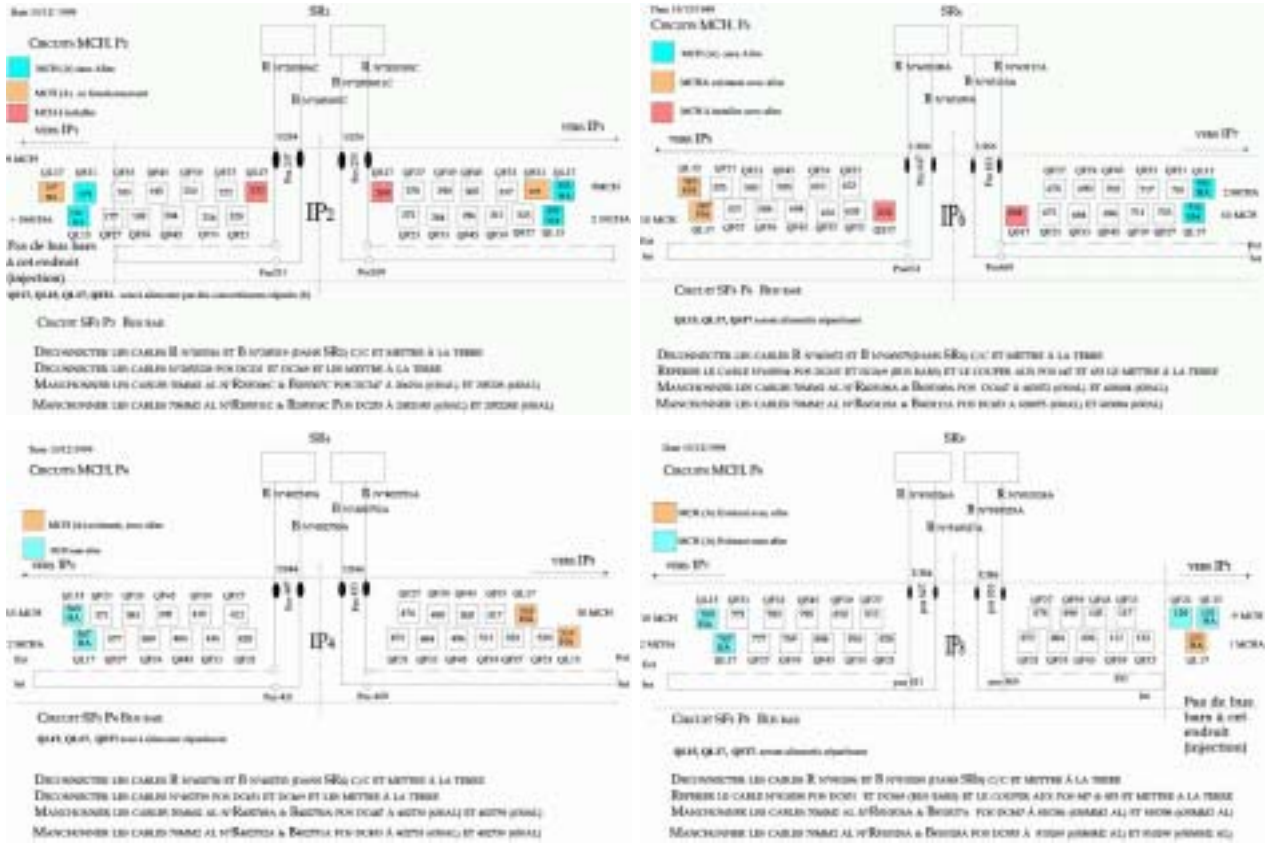

Figure 8: Cabling circuit for the MCH correctors in quarter sections of the machine

9 MCH current limits

The current for the individually powered MCH magnets is limited by the following factors :

- The heat load on the coil limits the current to 2.5 A. The limit might be increased by either accepting a higher operating temperature (to be tested) or by adding cooling to the coil.
- The maximum current of the power converters could be upgraded from 2.5 A to 5.0 A by changing a shunt resistor.
- The resistance of the circuits, 44Ω, and the available power converter voltage of 135 V limits the current to $3.07A$.

The current for the magnets which we will put in series via a bus bar is limited by :

- The heat load on the coil (see above).
- The resistance of the circuits and the available power converter voltages. The resistance in the ring of a bus-bar circuit with 10 MCH magnets connected is 232Ω. The power converter can deliver 600 V (could be upgraded to 700 V) giving a maximum current of 2.58 A (3.0 A).

In conclusion it is possible with some effort to upgrade the MCH systems from 2.5 A to 3.0 A but the achievable gain is very limited.

10 Manpower and material costs

The estimates costs for manpower and materials are given in table 7. To this we have to add the CERN staff (6 months PO engineer, 6 months MS technician, OP EIC, OP software update).

Connection of unused MCH		
	bus bar cabling	65 KCHF
	magnet connection pieces	30 KCHF
	magnet connection manpower	15 KCHF
	power convertor modifications	30 KCHF
	power cabling and installation in SR bld	80 KCHF
total		220 KCHF
Upgrade MCH current limits		
	magnet cooling upgrade	125 KCHF
	PC upgrade 2.5A-5A	50 KCHF

Table 7: Costs estimates of the BFS scheme for the final LEP run.

11 Conclusion

The LEP beam energy can be increased by spreading the bending field over the horizontal orbit correctors. To implement a good scheme 79 unused MCH correctors in the arcs and 14 unused MCH/MCHA correctors in the dispersion suppressors will be powered. With those additional correctors the orbit can be well corrected and an energy gain of approximatively 0.18 GeV could be obtained for a fixed RF volage.

References

[1] P. Raimondi, “Increasing the LEP energy for a given RF voltage”, Proc. of the IX Workshop on LEP-SPS Performance, CERN-SL-99-007 DI, February 1999.

[2] The LEP Design Report, Volume II, “The LEP main ring”, CERN-LEP/84-01, June 1984.

[3] S. Myers, “The LEP Collider, from design to approval and commisioning”, CERN 91-08, October 1991.

[4] M. Sands, “The physics of electron storage rings : an introduction”, SLAC-121, UC-28 (1970).